Journal of Sound and Vibration (2000) **231**(4), 1023–1037
doi:10.1006/jsvi.1999.2447, available online at http://www.idealibrary.com on IDEAL®

EXPERIMENTAL STUDY OF SMART SEGMENTED TRIM PANELS FOR AIRCRAFT INTERIOR NOISE CONTROL

S. M. Hirsch†, N. E. Meyer, M. A. Westervelt, P. King, F. J. Li, M. V. Petrova and J. Q. Sun

Department of Mechanical Engineering, University of Delaware, Newark, DE 19716, *U.S.A*

(*Received* 16 *October* 1998, *and in final form* 24 *May* 1999)

A smart trim panel used as a secondary source for active noise control in aircraft is developed and tested. The smart trim panel is a rectangular segment of aircraft trim panel which is suspended by a flexible support. This support converts the stiff trim panel into flexibly mounted pistons which can be driven by light-weight and low-profile force actuators. The smart trim panel has many advantages as an acoustic source over traditional loudspeakers: it is of lower profile, lower mass, and requires only a simple modification of materials already installed on aircraft. The static and dynamic properties of a smart trim panel are studied, verifying that when subjected to low-frequency (< 500 Hz) excitation, it vibrates in the efficiently radiating piston mode. Real-time active noise control experiments are conducted in a laboratory-scale fuselage model using the smart trim panels as secondary sources. Global attenuation of sound pressure levels of up to 15 dB is realized.

1. INTRODUCTION

A significant amount of research has been performed to develop active control technologies for quieting low-frequency noise in aircraft. Active noise control (ANC), which uses loudspeakers placed in the cabin as control sources, has been demonstrated to be an effective method [1, 2]. ANC systems typically can be implemented to control sound generated by any combination of disturbance sources. Active structural acoustic control (ASAC), which uses direct actuation on structural members to reduce their radiated sound, has also received much attention [3–10]. Fuller, Jones and Silcox report that ASAC provides effective control of noise radiated from vibrating elastic structures with fewer control actuators than required for comparable performance from an ANC system [9, 11]. Concern of fatigue damage to structures has lead many researchers to consider placing control actuators on non-critical structures, such as the interior trim panel [12–18]. The complicated vibration behavior of aircraft fuselage and trim panels makes it difficult to implement an ASAC system which controls sound radiated by

†Current address: The Boeing Company, PO Box 16858, Philadelphia, PA 19142, U.S.A.

0022-460X/00/141023 + 15 $35.00/0

all vibrating boundaries. It is often necessary to focus the structural control on a more local level, instead of attempting to control the entire structure. As a result, ASAC systems may leave many uncontrolled paths, known as flanking paths, for sound to radiate into the cabin.

To avoid problems of control spillover and high required actuation forces, others have considered segmentation of the vibrating boundary, either through the use of acoustic sources or structural modifications to convert the panel into stiff, lightweight sub-panels. Many researchers have studied a localized volume velocity control, in which the volume velocity of individual segments of a radiating boundary is cancelled [14, 19–25]. In general, one of the two methods has been employed. The first uses loudspeakers to generate the required 180° phase-shifted volume velocity to cancel the volume velocity of a region of the boundary. The second is to actuate directly on the sub-panels to minimize their volume velocity.

Much of the research in the works cited above is focused on active sound transmission control (ASTC), which is the application of active technologies to improve the transmission loss characteristics of a panel. Because of the existence of flanking paths for structural energy transmission in an aircraft, it may not be feasible to control all sound radiated into the cabin through the boundaries. It is important to preserve the ability to actuate directly on the acoustic medium to reduce noise levels due to sound not blocked by structural controls. Acoustic boundary control (ABC) is a new active control strategy for quieter aircraft developed by the authors [26–32]. ABC involves the distribution of light-weight, low-profile acoustic sources along the domain boundaries (i.e., the inside walls of an aircraft cabin). It has been shown that this approach provides advantages of both traditional loudspeaker-based systems and structural vibration control systems. A key component of this strategy is the so-called "smart" segmented trim panel—a segment of aircraft trim panel driven by a center-mounted control actuator. The goals of this study are to construct and study a prototype smart trim panel and to experimentally demonstrate the effectiveness of smart trim panels in a real-time active noise control system. The incorporation of the smart trim panel into an ASTC system is not studied; the results of studies by Sharp, St. Pierre, and Lieshman suggest that the smart trim panel design would be an effective implementation for ASTC [21, 22, 25].

Section 2 presents the design, construction, and preliminary testing of the smart trim panels. The piston mode resonant frequency of a smart trim panel is measured and compared with the predicted value based on static modelling. Tests are performed to verify that the low-frequency vibration of a smart trim panel is in the efficiently radiating piston mode. The smart trim panels are used as control sources in a real-time active noise control system in a laboratory-scale fuselage model. Section 3 presents the experimental configuration used for the real-time active noise control implementation. A summary of the results of the noise control experiments is presented in section 4. Sound-field distributions in the cylindrical enclosure are presented which compare the pressure levels before and after real-time active control is applied. The performance of smart trim panels and traditional loudspeakers as control sources is compared. The paper is concluded in section 5.

2. CONSTRUCTION AND PRELIMINARY TESTING

This section outlines the design, construction, and preliminary testing of the smart trim panels. A particular emphasis is placed on identifying the low-frequency vibration behavior. There are potentially three low-frequency modes of vibration for the smart trim panel: the piston mode (translation) and two rocking modes (rotation). For the smart trim panel to be an efficient acoustic radiator at low frequencies, it should vibrate in the piston mode. Rocking modes of a rigid panel correspond to an acoustic dipole, and do not radiate as efficiently as the piston mode at low frequencies.

2.1. SMART TRIM PANEL DESIGN

Three 0·165 m square segments are formed within a 0·635 m square section of a flat aircraft trim panel (Figure 1). A detailed lay-up view of the trim panel is shown in Figure 2. The trim panel has an effective Young's modulus of $8{\cdot}25 \times 10^{10}$ Pa, density of 335 kg/m^3, and thickness of 6·4 mm. The partition is created by carving grooves into the trim panel around each segment, leaving only the outer layer of fiberglass and Kevlar to connect the segment to the rest of the trim panel. This outer layer serves as a flexible support to the segment. The effects of groove widths on the support stiffness and on the vibration response of the segments are studied. The results reported in this section are based on the tests of a representative segment of actual dimension 0·162 m × 0·168 m. Note that in a real implementation,

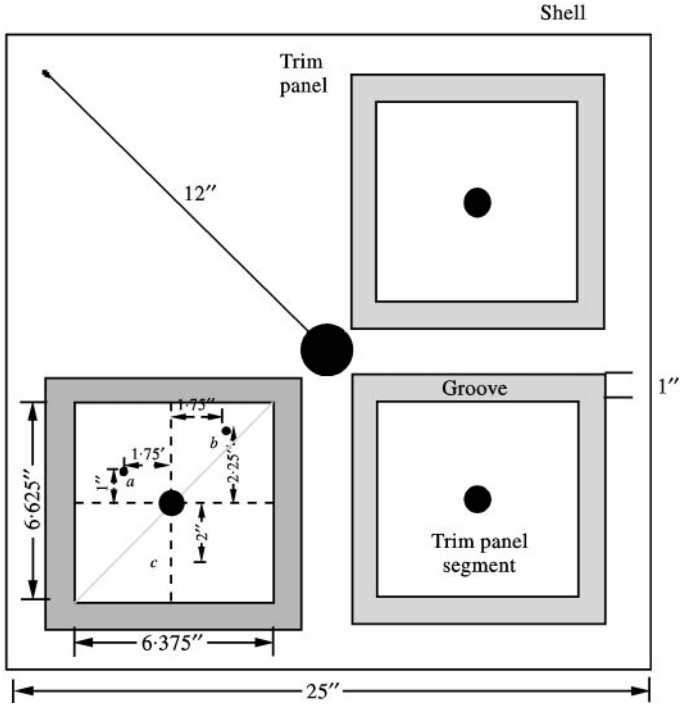

Figure 1. Schematic of a smart trim panel.

Figure 2. A typical lay-up of aircraft interior trim panel.

the flexible support of a segment should be created by a proper selection of material so that the resulting panel is smooth and continuous.

2.2. STATIC COMPUTATION OF SUPPORT STIFFNESS AND PISTON MODE RESONANT FREQUENCY

Static tests are performed to calculate the effective stiffness of the flexible support of the smart trim panel. This value is used, along with the known panel mass, to predict the resonant frequency of the piston mode, assuming that the trim panel behaves as a single degree-of-freedom harmonic oscillator. Static testing is performed with the trim panel assembly mounted vertically on a frame. A weight tray is hung from a string which is threaded through a small hole in the center of a panel segment and passed over a pulley. Deflection due to the addition of weight to the tray is measured with a Kanetec MB-BV dial indicator.

The panel deflection is measured as a function of applied force. The force–deflection curves for 6·4, 12·7, and 25·4 mm groove widths are presented in Figure 3. The effective support stiffness is computed with a first order curve fit. These values, along with the predicted piston-mode resonant frequencies, are also presented in Figure 3.

2.3. LOW-FREQUENCY VIBRATION RESPONSE CHARACTERISTICS

Dynamic tests are performed to measure the piston-mode resonant frequency. A force generator (Wilcoxon Research F5B electromagnetic mini shaker) is tightly screwed into a small hole in the center of the segment.

To determine its frequency response characteristics, the trim panel segment is structurally excited at its center with 1 kHz band-limited white noise. A piezoelectric accelerometer is placed at one of the three locations on the panel (marked by *a*, *b*, and *c* in Figure 1). The transfer function between the shaker input and the accelerometer output is recorded. The accelerometer response, normalized to the peak level at the lowest resonant frequency, is shown in Figure 4. Three curves are shown for each groove width: these are measured at the three locations. The predicted and measured resonant frequencies for the piston mode differ by about 5 per cent for the two smaller groove widths, but only one percent for the 25·4 mm groove.

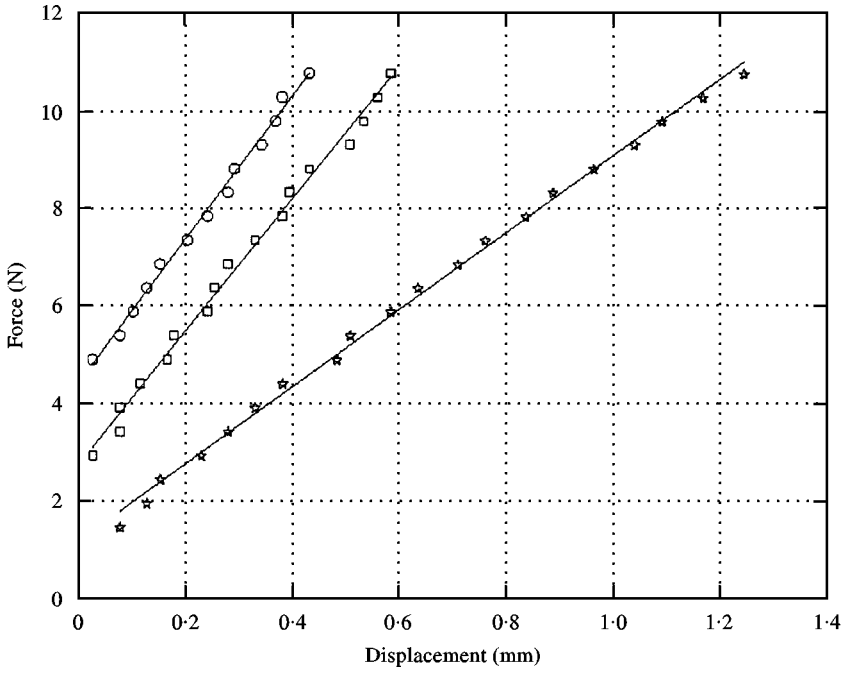

Figure 3. Force–deflection curves for segmented trim panel with different groove widths: –○–, groove width 6·4 mm, the predicted stiffness is 14·7 kN/m, and the predicted piston-mode resonant frequency is 41·25 Hz; –□–, groove width 12·7 mm, the predicted stiffness is 13·57 kN/m, and the predicted piston-mode resonant frequency is 40 Hz; –∗–, groove width 25·4 mm, the predicted stiffness is 7·8 kN/m, and the predicted piston-mode resonant frequency is 30 Hz.

Further analysis is performed on the accelerometer data measured with the 25·4 mm groove width, to determine if the piston-mode vibration of the panel segment occurs over a greater frequency bandwidth. The magnitude and phase of the sensor output, relative to the shaker input, are shown in Figure 5. Each plot contains three curves: these represent measurements taken at sensor locations *a*, *b*, and *c*. The sharp jumps in the phase data indicate phase wrapping between $\pm$ 180°.

The strong similarity between the three curves in each figure indicates that the panel segment is vibrating primarily in a piston mode over the entire frequency range presented. In particular, the result that the phase difference is mostly less than 45° is a strong indication that the rocking modes do not contribute significantly to the low frequency vibration. Presence of the two rocking modes would result in approximately 180° phase differences between measurement points *b* and *c* and/or *a* and *b*.

Assuming uniform support stiffness, the rocking modes are predicted to occur at resonant frequencies of 63·2 and 68·0 Hz. A peak in the vibration response is observed at 64 Hz. It is believed that this is due to a resonance of the shaker, not the rocking modes of the segmented trim panel, since the phase response at all three measurement locations undergoes nearly identical 180° phase shifts. The greatest disparity between the phase measurements occurs just below this frequency range, which is possibly due to the influence of rocking modes.

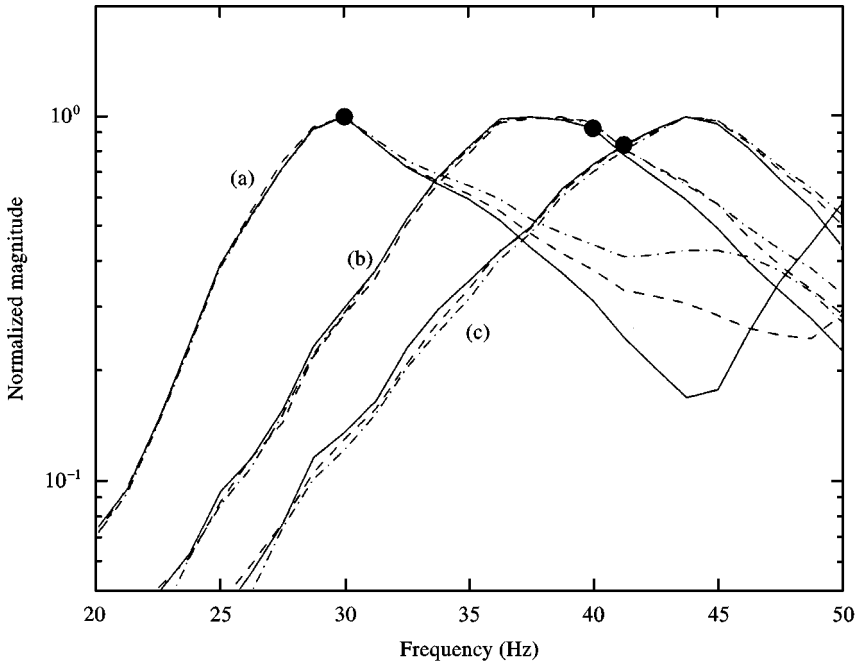

Figure 4. Identification of the piston-mode resonant frequency. For each panel, there are three measurements at locations *a*, *b*, and *c* as marked in Figure 1. (a) 25·4 mm groove (b) 12·7 mm groove (c) 6·35 mm groove; ●, indicates the predicted resonant frequency of the piston mode based on the static analysis.

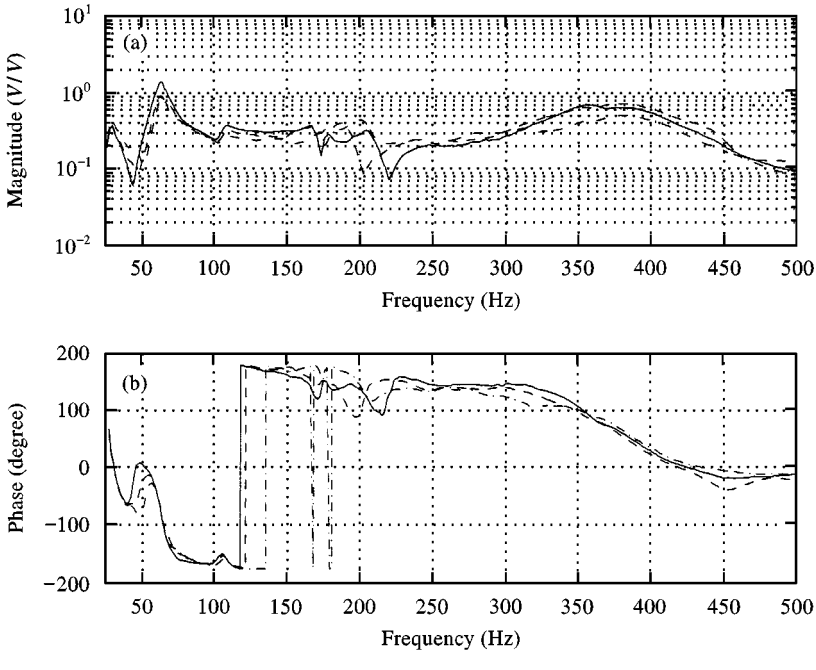

Figure 5. Vibration response of the segmented trim with a groove width 25·4 mm at multiple sensor locations: (a) Magnitude, (b) Phase; ——, location *a*; – · – · –, location *b*; – – – location *c*.

Furthermore, a ballpark estimate of the lowest resonant frequency for transverse vibration ((1,0) or (0,1) mode), obtained by modelling the smart trim panel as a simply supported square plate, is 1658 Hz, well above the frequency range of interest. These results suggest that the simple harmonic oscillator assumption should be valid for low frequencies. It should be noted that the frequency range for the targeted application is approximately 75–500 Hz.

3. ANC EXPERIMENTAL CONFIGURATION

3.1. SYSTEM GEOMETRY

Real-time active noise control experiments are conducted in a laboratory-scale fuselage model. The model, a cylindrical aluminum shell with closed ends, is shown in Figures 6 and 7. The end cap at $z = L_s$ is made of 38 mm thick pine; the end cap

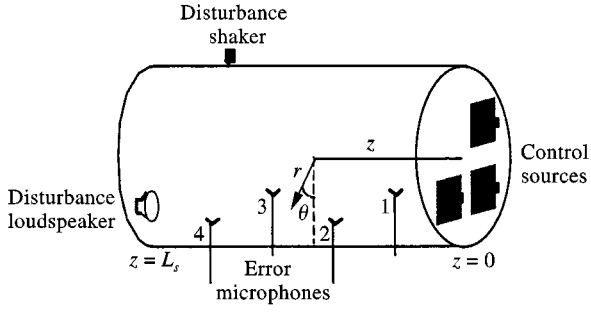

Figure 6. Geometry of experimental apparatus.

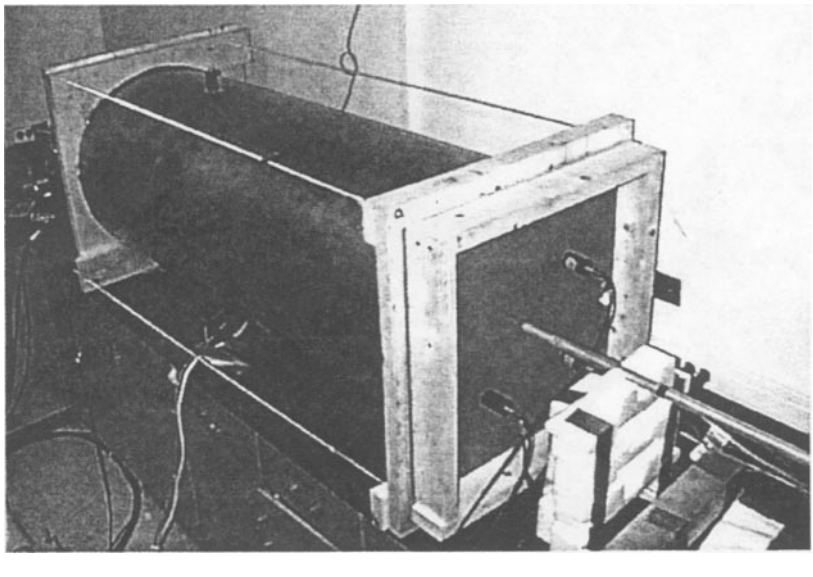

Figure 7. Exterior view of experimental apparatus.

at $z = 0$ is a flat sheet of aircraft trim panel with three smart trim panel segments for use as control sources (Figure 1). Each segment is excited by a center-mounted shaker (Wilcoxon Research F5B). The primary excitation of the system is either a shaker (also the F5B) glued to the shell at $\theta = 180^\circ$ and $z = 1{\cdot}128$ m (structural excitation) or a 10 cm diameter woofer mounted on the $z = L_s$ end cap centered at $\theta = 0^\circ$ and $r = 0{\cdot}23$ m (acoustic excitation). The woofer is replaced by a wooden plug for the tests when structural excitation only is considered, to preserve the approximately rigid boundary condition. The disturbance signal is generated with a digital signal generator. Four error microphones are placed in a horizontal plane inside the shell. The co-ordinates are $r = 0{\cdot}18$ m and $(z, \theta) = (0{\cdot}30\text{ m}, 45^\circ)$, $(0{\cdot}61\text{ m}, -45^\circ)$, $(0{\cdot}90\text{ m}, 45^\circ)$, $(1{\cdot}24\text{ m}, -45^\circ)$. A boom with two radially oriented arrays of six microphones each is supported by the two end caps. The microphone boom can be translated axially and rotated to allow for pressure measurements throughout the enclosure. Measurements are made every 180° circumferentially, 5 cm axially, and 4 cm radially, for a total of 3240 measurement points.

The normalized frequency response characteristics of the structure and of the acoustic field are indicated in Figure 8. The structural response data are presented as the sum of the squared measurements of four accelerometers placed on the shell, given broad-band excitation by disturbance shaker. The acoustic response data are the sum of the squared measurements of the four error microphones, given broad-band excitation by the disturbance loudspeaker. The sharp spikes in the acoustic response are 60 Hz measurement noise, not system resonances. The points

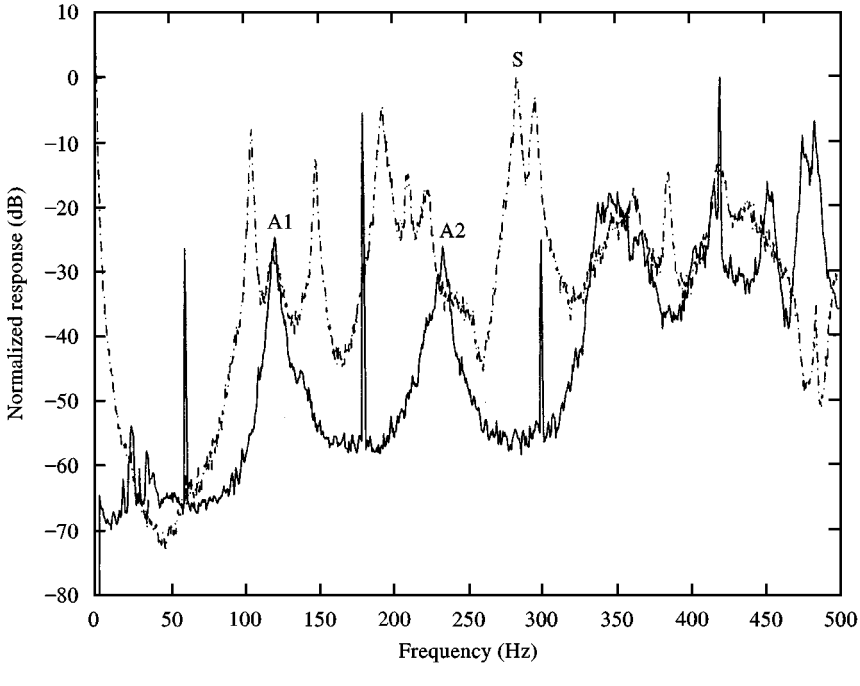

Figure 8. Frequency response of the cylindrical shell system. The sharp spikes at 60 Hz and its multiple are measurement noise –·–·–, Acoustic response; ——, structural response. Letters A1 and A2 represent the acoustic resonances. Letter S represents the structural resonance.

labelled A1, A2, and S are the first and second axial acoustic resonant frequencies and a dominant structural resonant frequency.

3.2. ACTIVE NOISE CONTROL SYSTEM

Active noise control is implemented using the leaky filtered-x LMS algorithm [33, 34]. The transfer functions from each actuator to each error sensor are represented at a given frequency as FIR filters with two coefficients. These coefficients are computed with an off-line system identification using the classical LMS adaptive digital filter. Each filter for the adaptive controller is implemented with two coefficients. The adaptive algorithm is computed with a sampling rate of 2200 Hz. A copy of the disturbance signal is used as a reference signal for the filtered-x algorithm. Control hardware limitations restrict the control system to two actuators and three error sensors.

The complete ANC experimental system is shown schematically in Figure 9. The adaptive controller is implemented on a dSPACE Digital Signal Processing Board (DS1102) interfaced with the MATLAB and Simulink programming environments. The r.m.s. values of the measurement microphone signals are acquired and computed with LabView. These measurements are used to generate the pressure maps and to compute global attenuation levels.

4. ANC EXPERIMENTAL RESULTS

Experiments focus on the ability of the smart trim panels to reduce interior sound pressure levels at 123 Hz, the first axial acoustic resonance. Both acoustic and structural disturbance sources are considered. Additionally, experiments are performed with standard 15 mm loudspeakers (Radio Shack Acoustic Suspension #40-1285D) replacing the smart trim panels as control sources. These experiments are performed to identify possible performance degradation resulting from the use of smart trim panels as control sources.

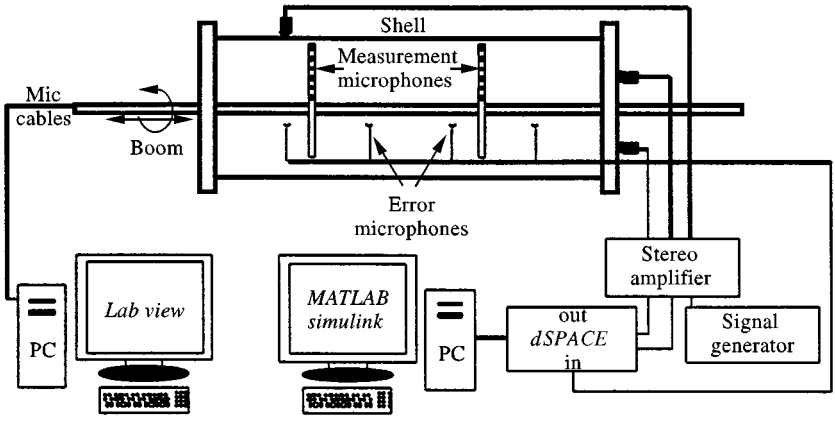

Figure 9. Schematic of control system configuration.

4.1. ACOUSTIC EXCITATION

We first present the control performance at 123 Hz, the first axial acoustic resonance, with the loudspeaker as the disturbance source (acoustic excitation). As numbered in Figure 6, control actuators $\#1$ and $\#3$, and error microphones $\#2$, $\#3$, and $\#4$ are used. The mean attenuation at the three error microphones is 14 dB; the global attenuation is 14·9 dB. The global attenuation is computed as the average attenuation observed at all 3240 measurement locations.

Figure 10 shows the pressure before and after control is applied at a radius of 0·12 m. The curve with smooth interpolated shading is the data before control. Recall that the disturbance source is at $z = L_s$ and the control actuators are at $z = 0$. This data demonstrates that the smart trim panels behave as required to significantly reduce the interior sound pressure levels. These results are typical for tonal control of a modal system at resonance: pressure levels at the loudest locations are greatly reduced, while levels at the quietest locations are increased slightly. The effect of the controller is to reduce the amplitude of the dominant mode. Additionally, we observe that the location of the pressure nodes is shifted, as a result of different impedance conditions at the end caps after control is applied.

4.2. STRUCTURAL EXCITATION

To simulate the challenges experienced in controlling a more complex sound field, we now consider the control performance when the primary sound field is

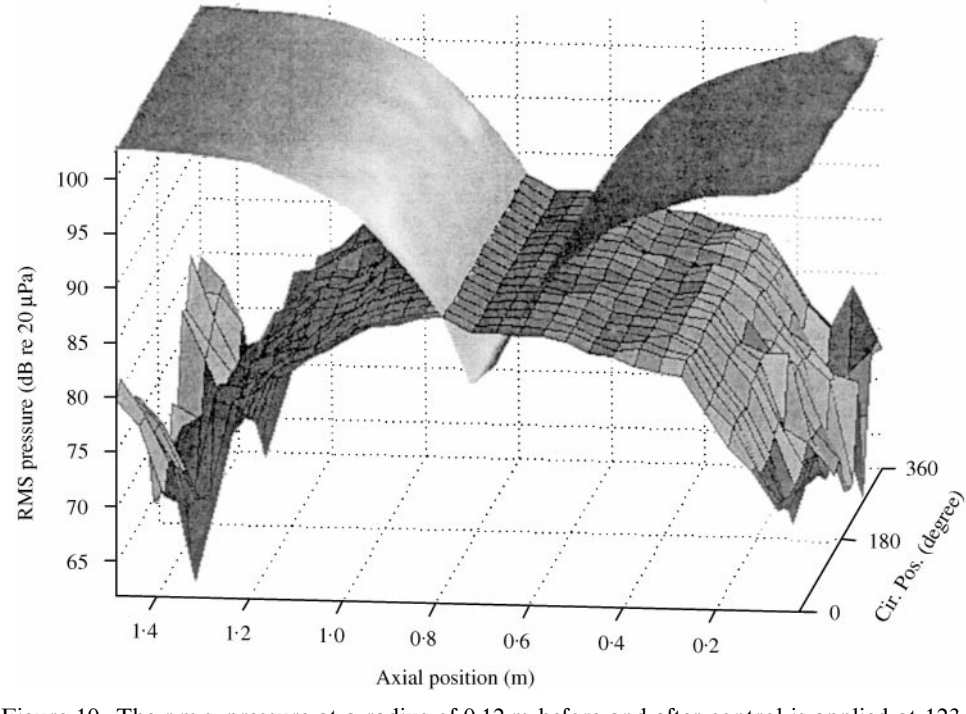

Figure 10. The r.m.s. pressure at a radius of 0·12 m before and after control is applied at 123 Hz (acoustic resonance). Acoustic excitation.

generated by structural excitation of the shell. Experimental results are again presented at the first axial acoustic resonant frequency. The actuator and microphone combinations are as before.

The sound field at 123 Hz and a radius of 0·12 m is shown in Figure 11. The mean attenuation at the three error microphones is 18 dB; the global attenuation is 10·1 dB. While the mode shape of the first axial acoustic resonance still dominates the uncontrolled pressure distribution, slight influences on the sound field of the structural vibration patterns are evident via the increased circumferential variation. As anticipated, the increased complexity in the sound field due to the structural excitation leads to a decrease in control performance. The sound field after control does not retain the modal characteristics of the sound field before control. While the controller reduces the amplitude of the dominant acoustic mode, it does not control the other acoustic modes which are excited by the structural vibration. Since this frequency is an acoustic resonance, the effects of the structural vibration are small.

The results of additional experiments are now reported. Control performance, given both structural and acoustic excitation of the second axial acoustic resonance (232 Hz) is studied. The global attenuation is 12 dB in both cases. The ability of this control system to reduce global pressure given structural excitation at a dominant structural resonant frequency (282 Hz) is also tested. While the pressure at the error microphones is reduced by an average of 5·7 dB, the global pressure increases by

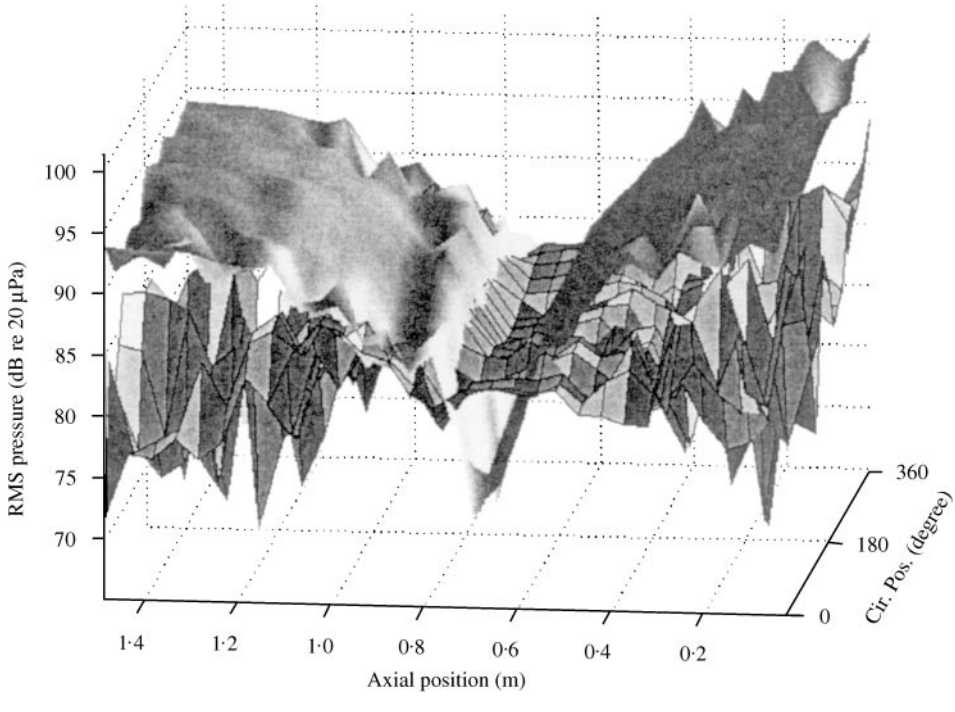

Figure 11. The r.m.s. pressure at a radius of 0·12 m before and after control is applied at 123 Hz (acoustic resonance). Structural excitation. Compare with Figure 10.

1·2 dB. This is due to the complexity of the sound field at this frequency relative to the dimension of the control system. To improve control performance in such a situation, it is suggested to consider either the use of a larger control system or ASAC.

4.3. CONTROL WITH TRADITIONAL LOUDSPEAKERS

The results of the previous sections demonstrate that smart trim panels can be used as control sources in an active noise control system. Since a goal of this research is to develop a new actuator which behaves as a loudspeaker, but with many additional desirable characteristics, it is necessary to demonstrate that the control performance with this actuator is comparable to that with loudspeakers. To this end, the first experiment is repeated, with 15 mm loudspeakers replacing the smart trim panels as control actuators.

The loudspeakers are mounted in the positions of control actuators #1 and #3. A sheet of trim panel is layered between the wooden end cap and an aluminum frame. The loudspeakers are mounted directly to the aluminium frame, aligned with holes in the trim panel. This configuration is employed to mimic the boundary (impedance) conditions of the original experiment to the greatest extent possible.

Results of this experiment are presented in Figure 12. The mean attenuation at the three error microphones is 16·3 dB; the mean attenuation observed throughout

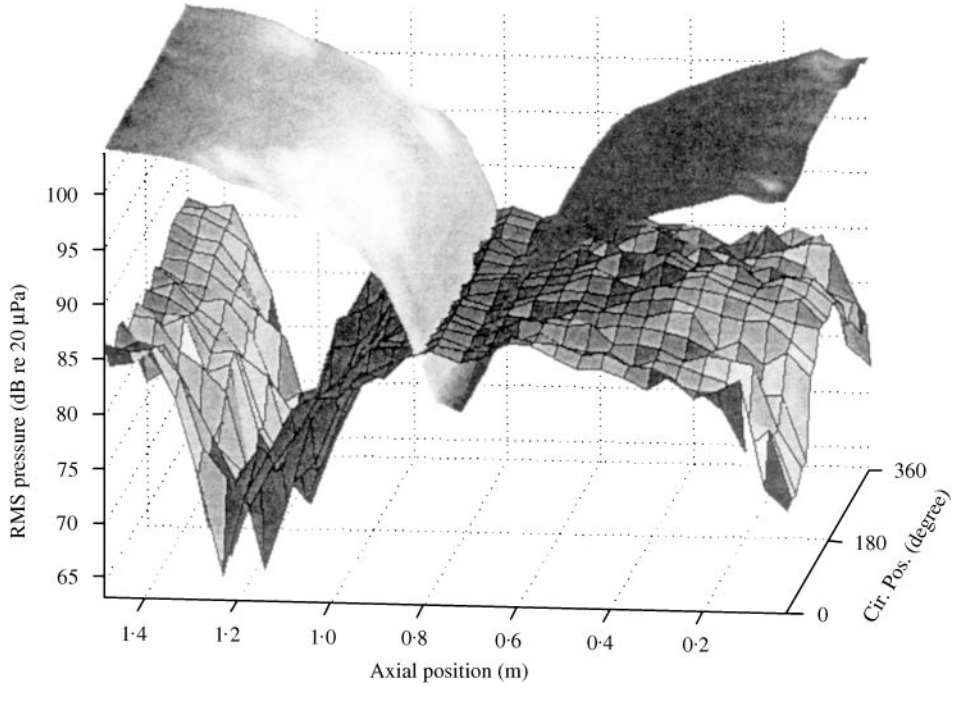

Figure 12. The r.m.s. pressure at a radius of 0·12 m before and after control is applied at a frequency of 123 Hz (acoustic resonance). Acoustic excitation. Loudspeakers used as control sources. Compare with Figure 10.

the enclosure is 15·53 dB. Comparison of Figure 12 with Figure 10 shows that the performance of smart trim panels is similar to that of conventional loudspeakers.

4.4. DISCUSSION OF EXPERIMENTAL RESULTS

The results presented in the previous sections indicate that the smart trim panels can be used instead of loudspeakers as acoustic sources in an active noise control system. A few further comparisons of these control sources are now made. A significant weight savings can be realized by replacing loudspeakers with smart trim panels. The weight of a single smart trim panel segment is 218 g, including the 160 g shaker. The weight of each loudspeaker used in these experiments is approximately 800 g.

Measurements of the acoustic efficiency indicate that the smart trim panel is approximately 1/100th as efficient as a loudspeaker. Despite this result, we were able to drive the smart trim panels with the same standard 100 W per channel power supply (Radio Shack MAP-200) used to drive the loudspeakers. It is also important to note that the smart trim panel design has not been optimized, while commercial speakers are highly optimized. Using a proper elastomeric mount to support the trim panel segments, and choosing a more efficient (and possibly lighter) shaker would drastically improve the acoustic efficiency of the smart trim panel.

5. CONCLUSION

A smart segmented trim panel for use in active noise control systems on aircraft has been developed and tested. It has been shown that the smart segmented trim panel is an effective, low-profile, low-mass acoustic source over the frequency range required of typical active noise control systems. Real-time active noise control is successfully implemented in a small cylindrical shell using the smart trim panels as secondary sources. The result of this work yields a novel acoustic actuator design for use with the acoustic boundary control method for reducing the sound pressure levels in aircraft. Two advantages of this design over traditional loudspeakers are its smaller mass and lower profile. Additionally, the installation of smart trim panels requires only a slight modification to existing materials on the aircraft.

ACKNOWLEDGMENTS

This work is supported in part by a grant (CMS-9634672) from the National Science Foundation and its supplementary support from the NSF Research Experience for Undergraduates (REU) program, and a grant from the State of Delaware Research Partnership program and Lord Corporation. Support by the Delaware Space Grant College Fellowship Program for S. M. Hirsch during the course of this work is also gratefully acknowledged. The authors would like to thank Rob Howes and Ralf Shepherd of Cessna Aircraft for providing trim panels and their material and geometrical properties, and for their support and endorsement of the project.

REFERENCES

1. A. J. Bullmore 1987 *Ph.D. Thesis, University of Southampton.* The active minimisation of harmonic enclosed sound fields with particular application to propeller induced cabin noise.
2. P. A. Nelson and S. J. Elliot 1992 *Active Control of Sound*. New York: Academic Press.
3. C. R. Fuller, R. J. Silcox, V. L. Metcalf, and D. E. Brown 1989 *Proceedings of the American Control Conference*, Vol. 3, 2079–2084. Experiments on structural control of sound transmitted through an elastic plate.
4. C. R. Fuller 1990 *Journal of Sound and Vibration* **136**, 1–15. Active control of sound transmission/radiation from elastic plates by vibration inputs I. Analysis.
5. C. R. Fuller, C. H. Hansen and S. D. Snyder 1991 *Journal of Sound and Vibration* **150**, 179–190. Experiments on active control of sound radiation from a panel using a piezoceramic actuator.
6. C. R. Fuller, C. H. Hansen and S. D. Snyder 1991 *Journal of Sound and Vibration* **145**, 195–215. Active control of sound radiation from a vibrating rectangular panel by sound sources and vibration inputs. an experimental comparison.
7. C. R. Fuller, S. D. Snyder, C. H. Hansen and R. J. Silcox 1992 *AIAA Journal* **30**, 2613–2617. Active control of interior noise in model aircraft fuselages using piezoceramic actuators.
8. C. R. Fuller and R. L. Clark 1992 *Proceedings of the fourth Aircraft Interior Noise Workshop*, 191–210. Sound transmission reduction with intelligent panel systems.
9. C. R. Fuller and R. J. Silcox 1992 *Journal of the Acoustical Society of America*, **91**, 519. Active structural acoustic control.
10. C. R. Fuller and G. P. Gibbs 1994 *Proceedings of 1994 National Conference on Noise Control Engineering* 389–394. Active control of interior noise in a business jet using piezoceramic actuators.
11. J. D. Jones and C. R. Fuller 1990 *The International Journal of Analytical and Experimental Modal Analysis* **5**, 123–140. Active control of structurally-cooupled sound fields in elastic cylinders by vibrational force inputs.
12. F. W. Grosveld, T. J. Coats, H. C. Lester and R. J. Silcox 1994 *Proceedings of the National Conference on Noise Control Engineering*. 403–408. Numerical study of active structual acoustic control in a stiffened, double wall cylinder.
13. R. J. Silcox, K. H. Lyle, V. L. Metcalf and D. E. Brown 1995 *Proceedings of the First Joint CEAS/AIAA Aeroacoustics Conference*, Vol. II, 1095–1104. A study of active structural acoustic control applied to the trim panels of a large scale fuselage model.
14. R. L. St. Pierre Jr., W. Chen and G. H. Koopmann 1995 *Proceedings of ASME Winter Annual Meeting*. Design of adaptive panels with high transmission loss characteristics.
15. D. R. Thomas, P. A. Nelson, S. J. Elliott and R. J. Pinnington 1993 *Noise Control Engineering* **41**, 273–279. Experimental investigation into the active control of sound transmission through stiff light composite panels.
16. B. N. Tran and G. P. Mathur 1996 *In Proceedings of the 1996 National Conference on Noise Control Engineering. Part* 1 (*of* 2), 395–400. Aircraft interior noise reduction tests using active trim panels.
17. K. H. Lyle and R. J. Silcox 1995 *Aerospace Engineering* **15**, 21–25. Active trim panels for aircraft interior noise reduction.
18. K. H. Lyle and R. J. Silcox 1996 *S. A. E. Transactions*, **104**, 180. A study of active trim panels for interior noise reduction in an aircraft fuselage.
19. B. V. Mason, K. Naghshineh and G. K. Toth 1994 *Proceedings of NoiseCon*, 467–472. Broadband, wide-area active control of sound radiation from vibrating structures using local surface-mounted radiation suppression devices.
20. B. V. Mason, G. K. Toth, K. Naghshineh and J. W. Kamman 1995 *Proceedings of ASME Winter Annual Meeting* 95-WA/NCA-8. A feedforward controller for active reduction of radiated noise from a uniformly vibrating circular plate.

21. R. L. St. Pierre Jr., G. H. Koopmann and W. Chen 1997 *Journal of Sound and Vibration* **210**, 441–460. Volume velocity control of sound transmission through composite panels.
22. S. J. Sharp, G. H. Koopman and W. Chen 1997 *Proceedings of NoiseCon*, 149–160. Transmission loss characteristics of an active trim panel.
23. M. E. Johnson and S. J. Elliott 1995 *Journal of the Acoustical Society of America* **98**, 2174–2186. Active control of sound radiation using volume velocity cancellation.
24. M. E. Johnson and S. J. Elliott 1997 *Journal of Sound and Vibration* **207**, 743–759. Active control of sound radiation from vibrating surfaces using arrays of discrete actuators.
25. T. W. Leishman and J. Tichy 1997 *Proceedings of NoiseCon*, 137–148. A fundamental investigation of the active control of sound transmission through segmented partition elements.
26. S. M. Hirsch and J. Q. Sun 1997 *Proceedings of The* 11*th VP*1*&SU Symposium on Structural Dynamics and Control*, 153–160. An acoustic boundary control method with actuator grouping for interior noise suppression.
27. S. M. Hirsch and J. Q. Sun 1997 *Proceedings of ASME* 16*th Biennial Conference on Mechanical Vibration and Noise*. Spatial characteristics of acoustic boundary control for interior noise suppression.
28. S. M. Hirsch and J. Q. Sun 1998 *Journal of the Acoustical Society of America* **104**, 2227–2235. Numerical studies of acoustic boundary control for interior sound suppression.
29. S. M. Hirsch and J. Q. Sun 1998 *Smart Materials and Structues*. Control signal scheduling for active noise control systems, to appear.
30. V. JayachANDRAN and J. Q. Sun 1998 *Smart Materials and Structures*, **7**, 72–84. Modelling shallow spherical shell piezoceramic actuators as acoustic boundary control elements.
31. V. Jayachandran, M. A. Westervelt, N. E. Meyer and J. Q. Sun 1998 *Smart Materials and Structures* **7**, 467–471. Experimental studies of shallow spherical shell piezoceramic actuators as acoustic boundary control elements.
32. J. Q. Sun and S. M. Hirsch 1997 *Proceedings of the SPIE Smart Structures and Materials*, Vol. 3041, 839–845. An acoustic boundary control method for interior noise suppression.
33. D. J. Rossetti, M. R. Jolly and S. C. Southward 1996 *Journal of the Acoustical Society of America* **99**, 2955–2964. Control effort weighting in feedforward adaptive control systems.
34. B. Widrow and S. D. Stearns 1985 *Adaptive Signal Processing*. Englewood Prentice-Hall. Cliffs, NJ.